JOURNAL OF GEOPHYSICAL RESEARCH, VOL. 93, NO. D12, PAGES 15,879–15,888, DECEMBER 20, 1988

On the Nonlinearity of the Tropospheric Ozone Production

X. LIN, M. TRAINER,[1] AND S. C. LIU

Aeronomy Laboratory, Environmental Research Laboratories, National Oceanic and Atmospheric Administration, Boulder, Colorado

The relationship of photochemical ozone production versus photochemical loss of an ozone precursor, that is, either NO_x or nonmethane hydrocarbons (NMHCs), is studied by using a box model with particular emphasis on the nonlinearity problem of the relationship with respect to the concentration of the precursor. Model calculations indicate that the composition of NMHCs, the ratio of NMHCs to NO_x, and the background concentrations of natural hydrocarbons, CO, and CH_4 all play important roles in determining the nonlinearity of O_3 production with respect to the loss of NO_x. In addition, influences on the nonlinearity due to radical loss via reactions of HO_2 with RO_2, exchanges between PAN and NO_2, and inclusion of nighttime NO_x loss processes are also investigated. Mechanisms that contribute to the nonlinearity are discussed. The nonlinear property of O_3 production versus loss of hydrocarbons and CO is different from that of NO_x. When the sum of CO and all hydrocarbons, including CH_4, natural NMHCs, and anthropogenic NMHCs, is used as the reference O_3 precursor, the nonlinearity is much less pronounced for ambient conditions usually found in rural air.

INTRODUCTION

In the troposphere the solar UV radiation does not have enough energy to dissociate O_2 directly and produce O_3. The existence of a high concentration of O_3 in the urban atmosphere prompted *Leighton* [1961] to suggest that peroxy radicals, such as HO_2 and RO_2 (where R denotes organic radicals), might lead to the oxidation of NO to NO_2, resulting in the production of O_3 following the photodissociation of NO_2. The peroxy radicals are produced mostly during the oxidation of hydrocarbons. Photochemical processes involved in O_3 production from oxidation of NMHCs are very complex [*Seinfeld*, 1986; *Finlayson-Pitts and Pitts*, 1986]. To facilitate later discussion, a highly simplified scheme is shown,

$$\text{NMHC} + \text{OH} + \text{O}_2 \rightarrow \text{RO}_2 \quad (1)$$

$$\text{RO}_2 + \text{NO} + \text{O}_2 \rightarrow \text{NO}_2 + \text{HO}_2 + \text{CARB} \quad (2)$$

$$\text{HO}_2 + \text{NO} \rightarrow \text{NO}_2 + \text{OH} \quad (3)$$

$$2(\text{NO}_2 + h\nu + \text{O}_2 \rightarrow \text{NO} + \text{O}_3) \quad (4)$$

$$\text{Net} \quad \text{NMHC} + 4\text{O}_2 + h\nu \rightarrow 2\text{O}_3 + \text{CARB} \quad (5)$$

where CARB stands for carbonyl compounds. Carbonyls undergo further oxidation and produce more O_3. The scheme shows that both NMHCs and NO_x ($NO + NO_2$) are precursors of O_3. It also shows that NO_x and odd hydrogen (OH + HO_2) are not consumed directly and thus act as catalysts in the production of O_3. Thus the production of O_3 usually increases with the concentrations of NO_x and odd hydrogen. In the absence of hydrocarbons, HO_2 can be produced via the reactions

$$\text{O}_3 + h\nu(<315\ \text{nm}) \rightarrow \text{O}(^1D) + \text{O}_2 \quad (6)$$

$$\text{O}(^1D) + \text{H}_2\text{O} \rightarrow 2\text{OH} \quad (7)$$

$$\text{OH} + \text{CO} \rightarrow \text{CO}_2 + \text{H} \quad (8)$$

and

$$\text{H} + \text{O}_2 + \text{M} \rightarrow \text{HO}_2 + \text{M} \quad (9)$$

In this scheme, CO replaces the NMHCs as an O_3 precursor. Of course, CH_4 can play the same role.

Because the destruction rates of NO_x and odd hydrogen depend strongly on the concentrations of NMHCs and NO_x, the increase of O_3 production is not linearly proportional to the increases in O_3 precursors. In fact, in certain circumstances O_3 production even decreases with increasing concentrations of the precursors. This nonlinear phenomenon is well known for the urban atmosphere and is readily shown by the O_3 isopleths of the Empirical Kinetic Modeling Approach (EKMA), which are used for formulating control strategies [*Dodge*, 1977*a*, *b*; *Dimitriades and Dodge*, 1983].

There is another way to look at the nonlinear O_3 production problem. Recently, *Liu et al.* [1987] defined an O_3 production efficiency defined as the number of O_3 molecules produced for each molecule of precursor consumed. They found that the nonlinearity of the efficiency is quite pronounced in the rural and clean background atmosphere and that this nonlinearity may have a significant impact on the budgets of regional and global O_3.

The composition of NMHCs and the ratios of NMHCs to NO_x used in the study by *Liu et al.* [1987] are those observed at Niwot Ridge, Colorado, a rural station. Three important questions are raised by their findings: (1) How sensitive is the nonlinearity with respect to the composition of NMHCs? (2) How does the ratio of NMHCs to NO_x affect the nonlinearity? (3) How do the background concentrations of natural hydrocarbons, CO, and CH_4, affect the nonlinearity? These questions will be investigated in this study.

In the following, a box model developed by *Liu et al.* [1987] with some modifications in the photochemical scheme, as described by *Trainer et al.* [1987] is used to study ozone production efficiency for various cases that correspond to different hydrocarbon compositions, ratios of NMHCs to NO_x, and mixtures of NMHCs, CO, CH_4, and natural hydrocarbons.

To study the dependence of the nonlinearity on the NMHC composition, model calculations with various realistic combinations of NMHCs are needed. However, constraint of computer resources requires models to incorporate only chemistry packages that include a limited number of hydrocarbons

[1]Also at Cooperative Institute for Research in Environmental Science, University of Colorado, Boulder.

Paper number 88JD03750.
0148-0227/88/88JD-03750$05.00

TABLE 1. Three NHMC Compositions Used in the Present Study

		Niwot		ADMP		EKMA	
	k_{CH}, $cm^3 s^{-1}$	Percent of Molecules	Percent in Carbon	Percent of Molecules	Percent in Carbon	Percent of Molecules	Percent in Carbon
Ethane	2.59(−13)	37.52	26.28	15.23	8.27		
Propane	1.14(−12)	21.27	22.35	5.97	4.86		
Butane	2.54(−12)	13.23	18.53	33.92	36.82	60.94	71.25
Ethylene	8.36(−12)	7.71	5.40	11.43	6.21		
Propene	2.71(−11)	2.68	2.82	5.46	4.45	27.08	23.75
Toluene	6.00(−12)	8.38	20.53	19.03	36.15		
Formaldehyde	1.00(−11)	6.70	2.35	5.97	1.62	6.84	2.00
Acetaldehyde	1.60(−11)	2.51	1.76	2.99	1.62	5.13	3.00
Reactivity K, $cm^3 s^{-1}$		3.75(−12)		5.33(−12)		8.93(−12)	

The reactivity of a composition is defined as the reaction rate constant weighted by the percentage of each component in carbon number. Read 2.59(−13) as 2.59×10^{-13}.

[*Lloyd et al.*, 1979; *Whitten et al.*, 1980, *Leone and Seinfeld*, 1985]. For this study we chose three NMHC compositions: (1) the rural composition observed at Niwot Ridge, Colorado [*Liu et al.*, 1987]; (2) the composition of a representative anthropogenic emission used by a regional acid deposition model [*Acid Deposition Modeling Project (ADMP)*, 1987]; and (3) the so-called "default EKMA" composition [*Dodge*, 1977*a*, *b*]. For simplicity, we will refer to these three NMHC compositions as Niwot, ADMP, and EKMA, respectively, in the text that follows. The components of each composition are listed in Table 1. It should be pointed out that our intention here is not to reproduce the ADMP and EKMA reaction schemes. The purpose is to have a diversified representation of NMHC mixtures in order to study the dependence of the nonlinearity on the NMHC composition. For simplicity, we have made the following adjustments on the ADMP composition. They are as follows: (1) dimethylbutane and xylene are treated as butane and toluene, respectively, and (2) butene is omitted. A comparison between O_3 calculated from our model with the adjusted ADMP composition and that calculated from the regional acid deposition model with the original ADMP composition is made. In these calculations the model starts at 0500 LT, with initial conditions of 30 parts per billion by volume (ppbv) of O_3, 1700 ppbv of CH_4, and 300 ppbv of CO. The initial NO_x varies from 0.1 to 1000 ppbv, while the initial anthropogenic NMHCs range from 1 ppbc (ppbv multiplied by carbon number) through 100,000 ppbc. The calculated O_3 values at noon time are presented in Figure 1. It is clear that the two sets of O_3 isopleths show a similar pattern of variations with NO_x and NMHCs. Some differences are expected, as the original ADMP mixture is more reactive. For example, at 10 ppbv of NO_x and 100 ppbc of NMHCs, our model with the adjusted ADMP composition generates 70 ppbv of O_3, whereas the corresponding value from the ADMP model and the original composition is 85 ppbv. The two O_3 values become 195 ppbv and 282 ppbv for NO_x at 100 ppbv and NMHCs at 1000 ppbc, respectively. The nonlinear phenomenon of the O_3 production is closely related to the relative O_3 variation with respect to changes in NO_x and NMHCs that are proportional to the space between isopleths, rather than the absolute value of the isopleth. Therefore differences in absolute O_3 values will not affect significantly the outcome of our study.

In addition to these investigations, effects on the nonlinearity of O_3 production due to combination reactions of HO_2 with RO_2 and the formation of peroxyacetyl nitrate (PAN) are studied. Since nighttime chemistry of NO_x is recognized to be important to the NO_x loss, hence the O_3 production, possible effects of the inclusion of nighttime chemistry on the nonlinearity are also discussed.

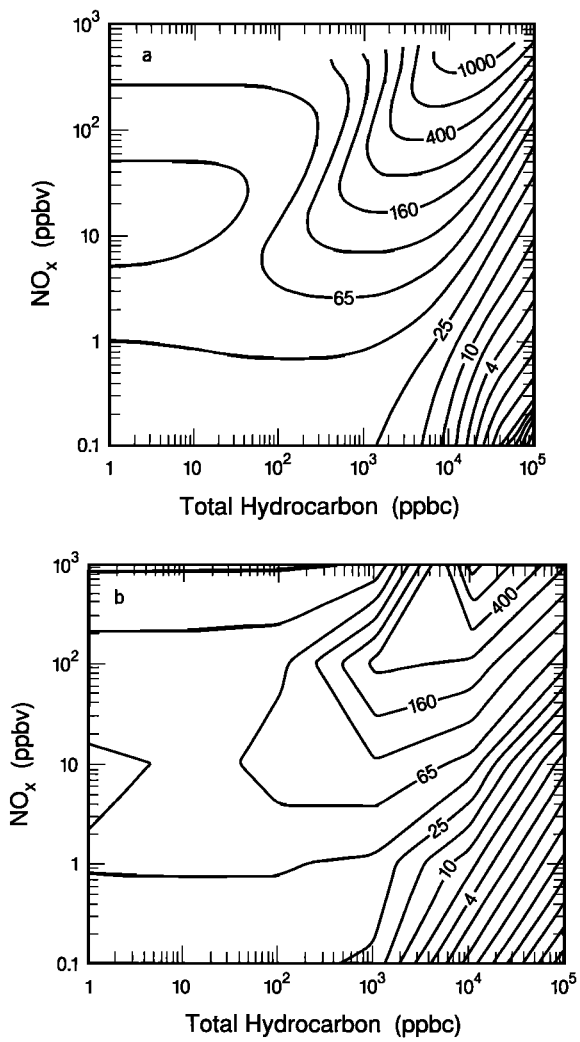

Fig. 1. Isopleths of O_3 mixing ratio (in ppbv) at noon, calculated from (*a*) the adjusted ADMP composition and the box model used in this paper; and (*b*) the original ADMP composition and the regional acid deposition model (W. Stockwell, private communication, 1988).

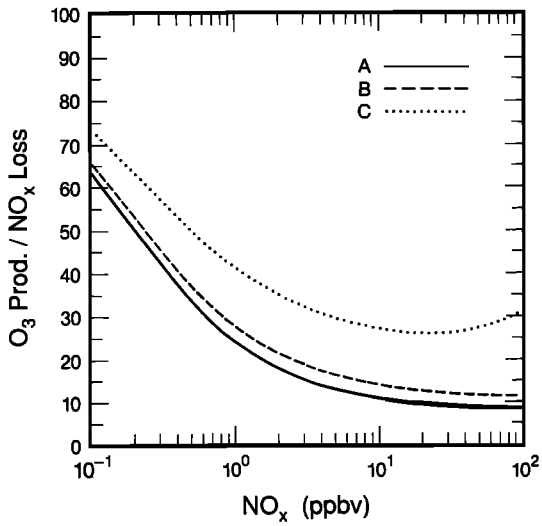

Fig. 2. O_3 production efficiency calculated by using the absolute O_3 production for three NMHC compositions: curve A, Niwot composition; curve B, ADMP composition; and curve C, EKMA composition.

NONLINEARITY AND THE HYDROCARBON COMPOSITION

In the troposphere the competition of (2) and (3), with the loss of odd nitrogen, determines how much O_3 is formed per NO_x consumed. Therefore it is crucial to understand the budgets of odd hydrogen and NO_x. The major NO_x loss during the daytime is

$$OH + NO_2 + M \rightarrow HNO_3 + M \quad (10)$$

In the presence of NMHCs, NO_x can also be converted into inactive forms, such as PAN, that do not produce O_3 directly. PAN is produced via the reaction

$$CH_3COO_2 + NO_2 + M \rightarrow PAN + M \quad (11)$$

At room temperature the reverse reaction is efficient enough that PAN and NO_2 tend to be in equilibrium. PAN may serve as a temporary storage and a carrier of NO_x into the more remote troposphere [*Crutzen*, 1979; *Singh et al.*, 1985]. In addition, NO_x may be lost at nighttime as a result of reactions involving NO_3 and N_2O_5 [*Ehhalt and Drummond*, 1982; *Platt et al.*, 1984; *Noxon*, 1983]. On the other hand, the reaction scheme (1)–(5) implies that in the absence of competing reactions, at least two O_3 molecules are formed following each reaction of OH with NMHC. Photochemical sinks for odd hydrogen include (10) and recombination reactions of HO_2 and RO_2 radicals

$$HO_2 + HO_2 \rightarrow H_2O_2 + O_2$$

$$HO_2 + RO_2 \rightarrow ROOH + O_2$$

followed by the reaction of OH with the peroxide. The preceding discussion indicates that interplay of the catalytic cycle and the radical loss reactions determines the production of O_3 with respect to the loss of its precursors. Because of the variation of the relative importance of the catalytic cycle versus the termination reactions that result in losses of precursors and odd hydrogen, the production of O_3 is not a linear function of the concentrations of its precursors.

Liu et al. [1987] discussed the finding that the total O_3 production in a region could be estimated from the total NO_x emission flux E within the region. This can be done by using a formula

$$S = EP/(L[NO_x])$$

where P and $L[NO_x]$ are the production of O_3 and the loss of NO_x, respectively. It is clear that a large uncertainty would result in the estimated total O_3 production if the value of $P/(L[NO_x])$ varies widely in the region of interest. Both the O_3 production and the NO_x loss vary with the level of NO_x and the composition and abundances of the other O_3 precursors, such as hydrocarbons. *Liu et al.* [1987] found that variations in the O_3 production and the NO_x loss are often similar and therefore cancel each other. This reduces substantially the uncertainty in the estimated total regional O_3 production. However, significant nonlinearity still exists.

In the preceding formula, NO_x is chosen as the reference precursor. This choice has two advantages: (1) The loss of NO_x on a regional scale is roughly equal to the emission flux, a result of the short photochemical lifetime of NO_x. (2) NO_x is the rate-limiting O_3 precursor in relatively clean air [*Fishman et al.*, 1979; *Logan et al.*, 1981]. Later, we will also discuss results from model calculations in which NMHCs are assumed to be the reference O_3 precursor.

The quantity $P/(L[NO_x])$ can be considered to represent the amount of O_3 produced for each NO_x molecule emitted, because in steady state the NO_x loss equals the NO_x emissions. We will call the quantity O_3 production efficiency.

It is important to note that the definition of absolute O_3 production and loss terms is not unique. It depends on how so-called "odd oxygen" is defined [*Liu*, 1977; *Fishman et al.*, 1979; *Levy et al.*, 1985]. On the other hand, the definition for net production of O_3 (i.e., photochemical production minus loss) is unique. Quantities calculated by using net production of O_3 are relatively easy to reproduce by other groups. In addition, the net production can be directly compared to the divergence of O_3 flux due to transport. In the following, the absolute O_3 production will be used only on one occasion, to calculate the O_3 production efficiency for the purpose of comparing results from this work with the results of *Liu et al.* [1987]. In the rest of the study, the net O_3 production will be used exclusively.

The nonlinearity of the ozone production efficiency obtained by *Liu et al.* [1987] (i.e., the Niwot case) is reproduced in profile A of Figure 2, using their definition of ozone production. It has essentially the same values as those of *Liu et al.* [1987]. Profiles B and C are the corresponding values for the ADMP composition and the EKMA composition, respectively. In these calculations the model is run for 5 days at first. During the 5-day period, O_3 is fixed at 40 ppbv, while NO_x is fixed at its specified levels (0.1 ~ 100 ppbv). The ratio of anthropogenic NMHCs to NO_x is taken as 23.4 ppbc/ppbv, the same value used by *Liu et al.* [1987]. This ratio is about a factor of 5 higher than the ratio in the emissions of anthropogenic NMHCs and NO_x. The higher ratio is expected for a rural site like Niwot Ridge as a result of the fact that NO_x is removed faster photochemically than most NMHCs. The levels of H_2O and CH_4 are fixed at 60% of relative humidity and 1600 ppbv of mixing ratio, respectively. The mixing ratio of CO is scaled to NO_x similarly to *Liu et al.* [1987]. This scaling gives 283 ppbv of CO at $NO_x = 0.5$ ppbv and 615 ppbv of CO at $NO_x = 10$ ppbv. We assume that natural hydrocarbons can be represented by isoprene and fix its value at a level of 0.1 ppbv. Nonzero initial values of the secondary hydrocarbons are specified only for formaldehyde and acetaldehyde. Their values are shown in Table 1. The diurnally changing photolysis rates are calculated for conditions at

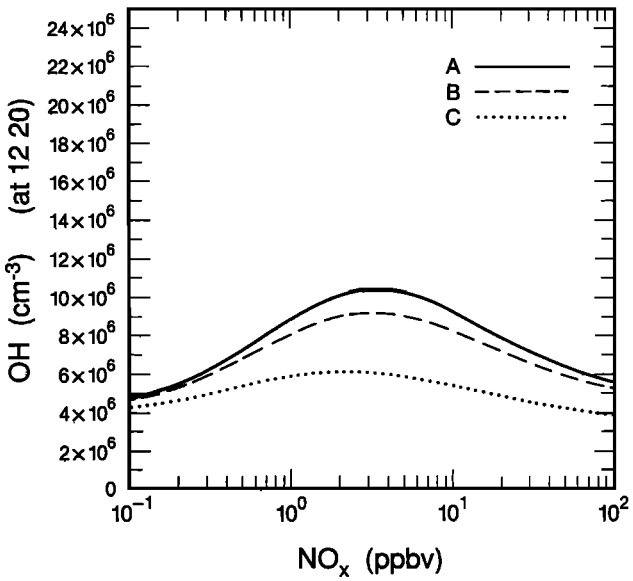

Fig. 3*a*. Same as Figure 2, except for concentration of OH.

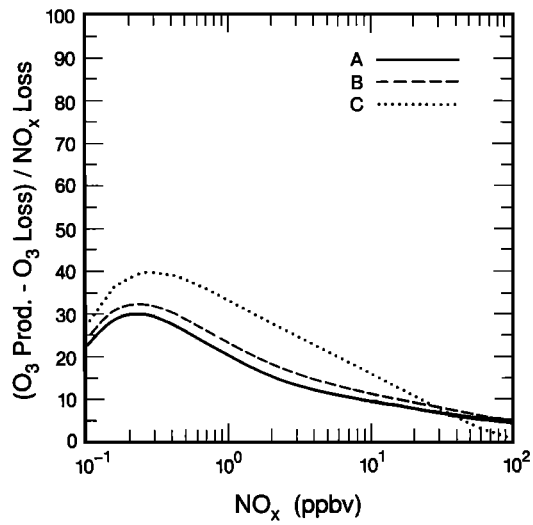

Fig. 4. O_3 production efficiency calculated by using the net O_3 production for three NMHC compositions: curve A, Niwot composition; curve B, ADMP coposition; and curve C, EKMA composition.

40°N on July 21 to represent the average summer solar insolation. The overhead ozone column density is fixed at 313 Dobson units and the ground albedo is assumed to be 10%. From 0500 LT on the sixth day, the O_3 mixing ratio is allowed to vary with time. All the results are taken from the sixth day. Since an approximate steady diurnal cycle is obtained from the first 5-day run, we omit the exchanges between PAN and NO_2 in calculating diurnally integrated production and loss for NO_x and O_3. This will be discussed in more detail later.

Comparison of the three profiles in Figure 2 shows that the nonlinearity of the O_3 production efficiency decreases with the reactivity of anthropogenic NMHCs when the efficiency is defined by using absolute O_3 production. For example, at 0.1 ppbv of NO_x, the differences in the O_3 production efficiency among the three cases are within 20%. In contrast, at 100 ppbv of NO_x, the ozone production efficiency for the EKMA case is about 4 times that of the Niwot case. This is reflected in the concentrations of OH and the sum of all peroxy radicals ($HO_2 + RO_2$), as shown in Figure 3*a* and Figure 3*b*, respectively. It is clear that higher reactivity of NMHCs leads to a higher concentration of $HO_2 + RO_2$, which tends to enhance the O_3 production. The increase in $HO_2 + RO_2$ reduces the nonlinearity by enhancing O_3 production at high concentrations of NO_x and NMHCs. The nonlinearity is reduced even further by the decrease of NO_x loss due to reduced concentrations of OH.

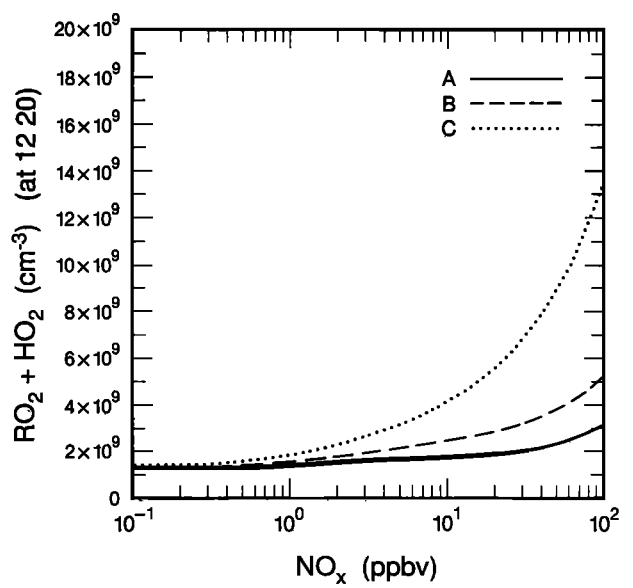

Fig. 3*b*. Same as Figure 2, except for concentration of $HO_2 + RO_2$.

When the net O_3 production is used to calculate the O_3 production efficiency, the results shown in Figure 4 are obtained. For the Niwot and ADMP compositions, the difference in the nonlinearity between Figure 4 and Figure 2 is small in the NO_x range from 0.4 to 10 ppbv. Below 0.4 ppbv of NO_x, the O_3 loss significantly suppresses the O_3 production efficiency, because the O_3 loss is almost independent of NO_x, while O_3 production is roughly proportional to NO_x [*Fishman et al.*, 1979; *Liu et al.*, 1983]. In fact, the ozone production efficiency becomes negative at NO_x levels lower than 80 parts per trillion by volume (pptv) as the O_3 loss becomes greater than O_3 production. When the NO_x level is greater than 10 ppbv, the O_3 production efficiency is also significantly affected by the inclusion of the O_3 loss, especially for the EKMA composition, in which a significant loss of O_3 occurs as a result of its reactions with propene. For the EKMA composition, at 100 ppbv of NO_x, which corresponds to 585 ppbc of propene, the O_3 production efficiency is a factor of 30 smaller with the O_3 loss included than that without the O_3 loss. Because of the large reduction of O_3 production efficiency at high NO_x levels as the O_3 loss is included, the overall nonlinearity is enhanced for all three hydrocarbons compositions. For the EKMA case the ratio of O_3 production efficiency at 1 ppbv NO_x to that at 100 ppbv NO_x is greater than 40 in Figure 4, whereas the ratio is only about 1.4 in Figure 2. Contrary to Figure 2, an overall increase of the nonlinearity of the O_3 production efficiency with the reactivity of the hydrocarbon mixture is clearly demonstrated from Figure 4. Some detailed results from model runs are presented in Table 2 for the three NMHC compositions. One can see that at low NO_x levels (e.g., below 1 ppbv), increase of the NMHC reactivity enhances the O_3 production efficiency

TABLE 2. Twenty-Four Hour Accumulated NO_x Loss, Ozone Production, Ozone Loss, Ozone Loss Due to O_3 Plus Ethene, and Ozone Loss Due to O_3 Plus Propene at Various NO_x Levels for Three NMHC Compositions

	Niwot NMHC Composition	ADMP NMHC Composition	EKMA NMHC Composition
	NO_x = 0.1 ppbv		
NO_x loss	2.92(9)	2.87(9)	2.66(9)
O_3 production	1.86(11)	1.89(11)	1.96(11)
O_3 loss	1.21(11)	1.21(11)	1.24(11)
O_3 loss due to O_3 + ethylene	1.97(8)	2.18(8)	0
O_3 loss due to O_3 + propene	4.76(8)	7.24(8)	4.07(9)
	NO_x = 1 ppbv		
NO_x loss	6.15(10)	5.72(10)	4.32(10)
O_3 production	1.48(12)	1.59(12)	1.79(12)
O_3 loss	2.54(11)	2.71(11)	3.58(11)
O_3 loss due to O_3 + ethylene	3.66(9)	4.20(9)	0
O_3 loss due to O_3 + propene	8.84(9)	1.40(10)	8.26(10)
	NO_x = 10 ppbv		
NO_x loss	7.36(11)	6.89(11)	4.87(11)
O_3 production	8.03(12)	9.67(12)	1.33(13)
O_3 loss	1.31(12)	1.87(12)	5.39(12)
O_3 loss due to O_3 + ethylene	1.24(11)	1.61(11)	0
O_3 loss due to O_3 + propene	3.00(11)	5.32(11)	3.43(12)
	NO_x = 100 ppbv		
NO_x loss	5.04(12)	4.93(12)	3.83(12)
O_3 production	4.28(13)	5.72(13)	1.19(14)
O_3 loss	2.10(13)	3.45(13)	1.16(14)
O_3 loss due to O_3 + ethylene	4.51(12)	5.93(12)	0
O_3 loss due to O_3 + propene	1.08(13)	1.96(13)	9.47(13)

Production and loss are given in units of cm^{-3} s^{-1}; NMHC is scaled to NO_x by 23.4. Read 2.93(9) as 2.93×10^9.

through both increased O_3 production and decreased NO_x loss. On the other hand, at higher NO_x levels increase of the reactivity reduces the O_3 production efficiency because of increased O_3 loss, mostly due to the O_3 reaction with alkenes.

The dependence of the nonlinearity on the ratio of NMHCs to NO_x is studied by varying the ratio over a wide range in the model calculations. O_3 production efficiencies for seven cases, corresponding to ratios of 0.3, 1, 4, 23.4, 50, 100, and 300, respectively, are plotted in Figure 5 for the ADMP composition. This range of the ratio more than covers the values found in rural and urban atmospheres, according to a survey by *Stockwell et al.* [1988]. The degree of nonlinearity remains large for all cases. It is seen that below 10 ppbv of NO_x, the O_3 production efficiency increases with the ratio of NMHCs to NO_x. The increase of the efficiency is due to the combined effect of smaller OH concentration and greater $HO_2 + RO_2$ concentration. However, when NO_x is above 10 ppbv, a tendency for the efficiency to decrease with the ratio becomes apparent. This is because the higher ratio leads to greater O_3 loss through its reaction with alkenes and, consequently, suppresses its production efficiency. This is similar to the results shown in Figure 4. Therefore there is a stronger nonlinearity of the O_3 production efficiency at high NMHCs/NO_x ratios. We also calculated the variation of the O_3 production efficiency with respect to various NMHCs/NO_x ratios for the Niwot and EKMA compositions. The results showed patterns similar to the ADMP case.

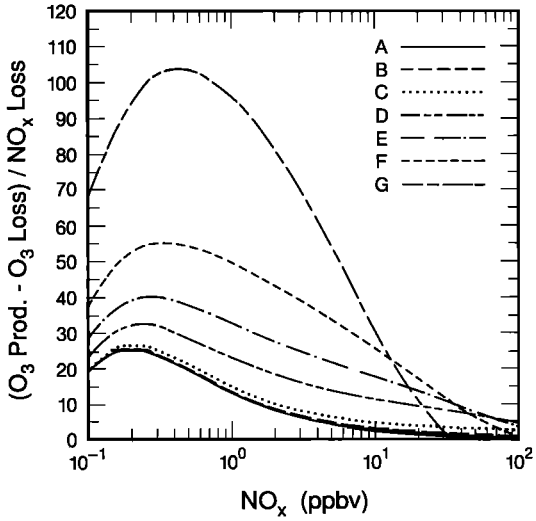

Fig. 5. O_3 production efficiency calculated from the ADMP composition for various NMHCs/NO_x (ppbc/ppbv) levels: curve A, 0.3; curve B, 1; curve C, 4; curve D, 23.4; curve E, 50; curve F, 100; curve G, 300.

When levels of atmospheric NMHCs are low, the O_3 production efficiency depends on levels of CO, CH_4 and natural hydrocarbons. Consequently, the nonlinearity will depend on the levels of those species. Figure 6 shows results from four model runs for the ADMP composition. Curve A shows a baseline run with standard ADMP composition (i.e., curve D in Figure 5); curve B, a run with isoprene removed; curve C, a run with isoprene and CH_4 removed; and curve D, run with isoprene, CH_4 and CO removed. As expected, the O_3 production efficiency decreases when isoprene, CH_4, and CO are

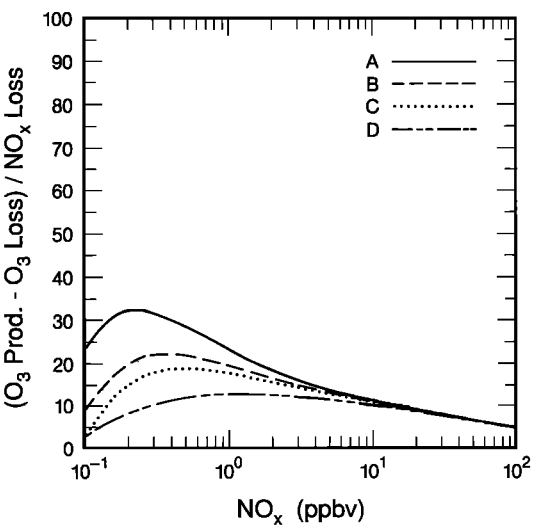

Fig. 6. O_3 production efficiency calculated from (curve A) the baseline run, (curve B) run with isoprene removed, (curve C) run with isoprene and CH_4 removed, and (curve D) run with isoprene, CH_4, and CO removed, respectively.

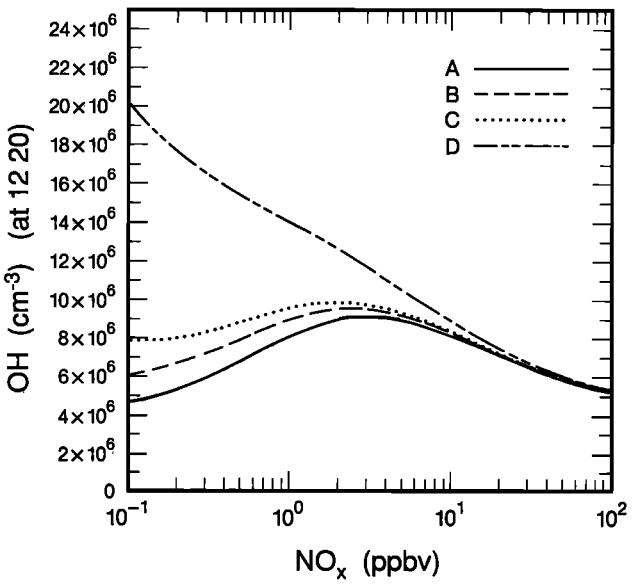

Fig. 7a. Same as Figure 6, except for concentration of OH.

removed. It is interesting to note that the O_3 production efficiency is essentially linear when isoprene, CO, and CH_4 are absent and NMHCs are linearly scaled to NO_x. The change of O_3 production efficiency in the four model runs can be understood by examining the concentrations of OH and HO_2 + RO_2, as plotted in Figure 7. A noticeable feature in Figure 7a is the major role that CO plays in suppressing the abundance of OH at NO_x levels below 1 ppbv. The change in OH leads to a change in the NO_x sink through the reaction of NO_2 with OH, and consequently, a change in the O_3 production efficiency. However, as we can see from Figure 6, the variation of the O_3 production efficiency does not show an abrupt shift from curve C to curve D at low NO_x levels. This is because a more efficient supply of RO_2 from NMHCs than of HO_2 from CO elevates the total amount of $HO_2 + RO_2$ and thus partly compensates for the relatively large change in NO_x loss between curve C and curve D. Results from other model runs show that this also applies to Niwot and EKMA cases.

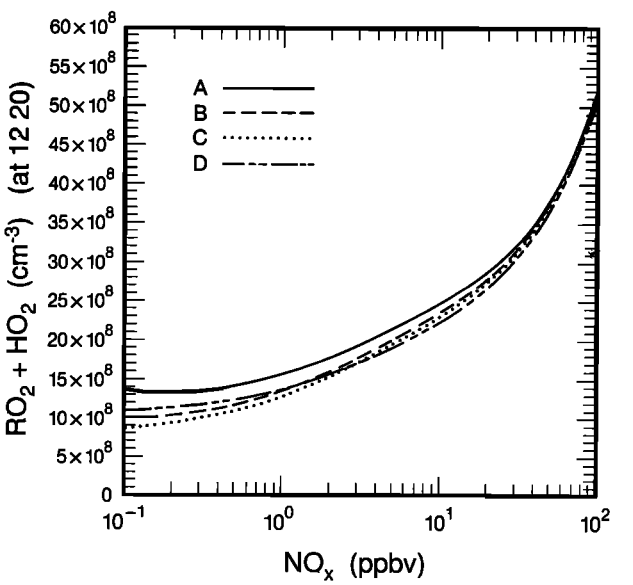

Fig. 7b. Same as Figure 6, except for concentration of $HO_2 + RO_2$.

TABLE 3. Twenty-Four Hour Accumulated Ozone Production, Ozone Loss, NO_x loss, and 24-Hour Averaged Ozone Production Efficiency and Concentrations of OH, HO_2, and $RO_2 + HO_2$ at 1220 for Various NO_x Levels and for ADMP NMHC Composition

	Baseline Run	Same, But Excluding Reactions of $RO_2 + HO_2$	Same, but Including Exchanges Between Pan and NO_x
	NO_x = 0.1 ppbv		
O_3 production	1.89(11)	2.40(11)	2.29(11)
O_3 loss	1.21(11)	1.32(11)	1.61(11)
O_3 net production	6.79(10)	1.08(11)	6.78(10)
NO_x loss	2.87(9)	2.88(9)	2.86(9)
O_3 production efficiency	23.7	37.5	23.7
OH	4.63(6)	4.42(6)	4.63(6)
HO_2	6.13(8)	7.20(8)	6.13(8)
$RO_2 + HO_2$	1.37(9)	1.93(9)	1.37(9)
	NO_x = 1 ppbv		
O_3 production	1.59(12)	1.71(12)	2.14(12)
O_3 loss	2.71(11)	2.94(11)	8.36(11)
O_3 net production	1.32(12)	1.42(12)	1.30(12)
NO_x loss	5.72(10)	5.95(10)	5.72(10)
O_3 production efficiency	23.1	23.9	22.8
OH	8.06(6)	8.24(6)	8.06(6)
HO_2	8.96(8)	9.85(8)	8.93(8)
$RO_2 + HO_2$	1.55(9)	1.74(9)	1.54(9)
	NO_x = 10 ppbv		
O_3 production	9.67(12)	1.01(13)	2.02(13)
O_3 loss	1.87(12)	2.00(12)	1.28(13)
O_3 net production	7.83(12)	8.07(12)	7.41(12)
NO_x loss	6.89(11)	7.12(11)	6.91(11)
O_3 production efficiency	11.4	11.4	10.7
OH	8.22(6)	8.46(6)	8.24(6)
HO_2	1.34(9)	1.44(9)	1.33(9)
$RO_2 + HO_2$	2.45(9)	2.62(9)	2.41(9)
	NO_x = 100 ppbv		
O_3 production	5.72(13)	5.87(13)	1.84(14)
O_3 loss	3.45(13)	3.63(13)	1.66(14)
O_3 net production	2.27(13)	2.25(13)	1.86(13)
NO_x loss	4.93(12)	5.09(12)	4.94(12)
O_3 production efficiency	4.60	4.42	3.76
OH	5.25(6)	5.36(6)	5.26(6)
HO_2	3.01(9)	3.16(9)	2.79(9)
$RO_2 + HO_2$	5.16(9)	5.43(9)	4.76(9)

Production and loss are given in units of cm^{-3} s^{-1}; production efficiency is given in units of molecules of ozone produced per NO_x molecule consumed; concentration is given in units of cm^{-3}; NMHC is scaled to NO_x by 23.4) Read 1.89(11) as 1.89×10^{11}.

As stated earlier, in our calculations conversions between PAN and NO_2 are omitted because the diurnally integrated conversion rates are nearly equal and cancel each other in most cases. It is important to check the accuracy of this assumption. In Table 3 a comparison of the baseline run and a run with the conversion terms included for the ADMP hydrocarbon composition is presented. It is clear that inclusion of the exchanges does not significantly affect the net O_3 production. Even at a high level, such as NO_x = 100 ppbv, the effect is limited to 20%. When the exchanges between PAN and NO_2 are included, the increase in O_3 production is almost canceled by the increase in the O_3 loss, which indicates that a

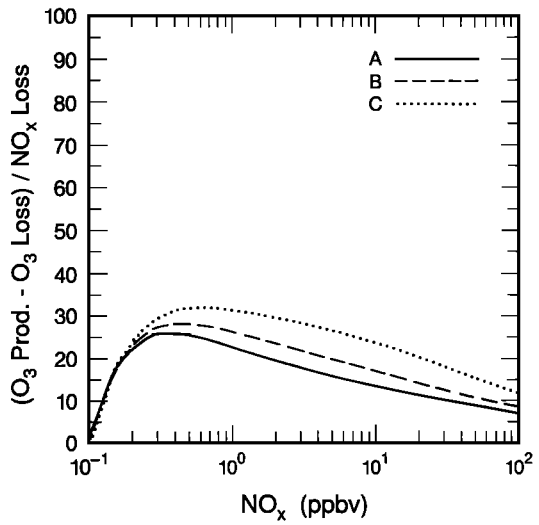

Fig. 8. Calculated O_3 production efficiency for three initial NMHC compositions: curve A, Niwot composition; curve B, ADMP composition; and curve C, EKMA composition. NMHCs and NO_x are time-dependent in the calculation.

quasi-chemical steady state in the conversion is reached after the initial 5-day run. In fact, for low NO_x (e.g., less than 1 ppbv) a run with less than 5 days is enough to reach such a quasi-steady state. If we regard the part of NO_x transformed into the form of PAN as a loss of NO_x, the nonlinearity of the O_3 production efficiency will be enhanced, because the PAN formation becomes comparable to and greater than the NO_x loss through the OH and NO_2 reaction as the NO_x level increases. For example, in the case of ADMP composition, the daily gain of PAN is only 7% of the diurnally integrated rate of the OH and NO_2 reaction at 0.1 ppbv of NO_x, whereas the former is 2 times the latter at 100 ppbv of NO_x. However, PAN acts as a temporary reservoir for NO_x, and the part of NO_x that is in the form of PAN will eventually be converted back to NO_x. Therefore we have chosen to exclude the PAN formation from the NO_x loss.

In calculations we have made so far, the concentrations of NO_x and NMHCs are held constant. These conditions are appropriate for a steady state situation in which the losses of NO_x and NMHCs are replenished by emissions or transport. Another way to investigate the problem is to view it as an initial value problem; that is, values of NO_x and NMHCs are calculated in the continuity equations from their initial values. This approach was taken in creating the isopleths in Figure 1 and is the approach traditionally adopted by the EKMA control strategy. Figure 8 illustrates the O_3 production efficiencies plotted against initial NO_x for the Niwot, the ADMP, and the EKMA compositions. Here initial NHMCs are scaled to the initial NO_x with a factor of 23.4, as before. In these calculations, NO_x and NMHCs are computed by assuming no emission sources and therefore decrease with time. The profiles in Figure 8 should be compared to those of Figure 4. The degree of nonlinearity of Figure 8 is substantially smaller than that in Figure 4. This is expected because the O_3 production efficiency is a value integrated over a day and thus represents an averaged quantity. Since photochemical lifetimes of reactive hydrocarbons and NO_x are short compared to a day, the O_3 production efficiency for certain initial NO_x and NMHC levels represents a value averaged over a wide range of NO_x and NMHC concentrations. For example, in the case of the ADMP composition, an initial 100 ppbv of NO_x at 0500 LT will result in 42 ppbv of NO_x, 39 ppbv of HNO_3, and 19 ppbv of PAN at noon. In addition, there is another factor involved in reducing the nonlinearity of O_3 production efficiency, that is, the changing NMHCs to NO_x ratio. Our model calculations indicated that the ratio generally increases with time in the initial value mode. Therefore the value of O_3 production efficiency is also averaged over a range of NMHCs to NO_x ratios. These two averaging procedures suppress the nonlinearity of O_3 production efficiency.

EFFECTS OF UNCERTAINTY IN PHOTOCHEMISTRY

There are significant gaps and uncertainties in our understanding and treatment of the photochemistry. It is not practical to quantify all of the uncertainty factors of the nonlinearity of O_3 production efficiency. In the following, however, we will examine the effects on the nonlinearity due to two major uncertainties in the photochemistry, namely, combination reactions of RO_2 with HO_2 and the nighttime sink of NO_x.

In our model runs the combination reactions of RO_2 with HO_2 are included. These reactions have significant impact on abundances of HO_2 and RO_2 radicals and hence the O_3 production efficiency. However, reaction rates and products formed in these reactions are still quite uncertain at the present time. In the model, we adopt a value of $7.7 \times 10^{-14} \times \exp(1300/T)$ cm^3 s^{-1} for the HO_2 reaction with CH_3O_2, as recommended by the Jet Propulsion Laboratory [*DeMore et al.*, 1985], and a value of 3×10^{-12} cm^3 s^{-1} for reactions of HO_2 with all other higher RO_2, as recommended by *Atkinson and Lloyd* [1984]. As for the products of the reactions, we take CH_3OOH as the surrogate. To examine the effect of these combination reactions on the nonlinearity of O_3 production, we ran the model without the combination reactions of HO_2 and RO_2. Model results corresponding to the ADMP composition case are presented in Table 3. One can see that exclusion of HO_2 reactions with RO_2 increases peroxy radical concentrations, especially at low NO_x levels. At these levels the combination reactions compete with reactions of peroxy radicals and NO in converting the radicals [*Carter et al.*, 1979].

As for the O_3 production efficiency, the value is increased at NO_x levels below 1 ppbv when the combination reactions are removed. For example, the efficiency is increased by 58% at $NO_x = 0.1$ ppbv. On the other hand, when NO_x is above 10 ppbv, the efficiency is only slightly changed. This pattern is also valid for the Niwot and EKMA cases. In summary, the role played by the combination reactions of HO_2 with RO_2 in a photochemical system is to reduce the overall nonlinearity of O_3 production efficiency, mainly through suppressing the efficiency at NO_x levels below 1 ppbv.

Another uncertainty in the chemistry that may significantly affect the O_3 production efficiency is the nighttime chemistry of NO_x. During the night, NO_2 is converted to NO_3 and N_2O_5 through reactions

$$NO_2 + O_3 \rightarrow NO_3 + O_2 \quad (12)$$

$$NO_2 + NO_3 + M \rightarrow N_2O_5 + M \quad (13)$$

This process is followed immediately by the thermal decomposition of N_2O_5:

$$N_2O_5 + M \rightarrow NO_2 + NO_3 + M \quad (14)$$

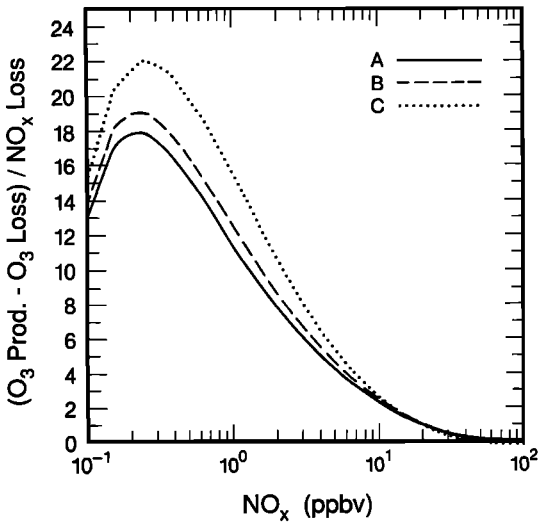

Fig. 9. Same as Figure 4, except for reaction of NO_2 with O_3 treated as a nighttime NO_x loss.

TABLE 4. Twenty-Four Hour Averaged Ozone Production Efficiency Calculated With and Without NO_2 plus O_3 With and Without Nighttime NO_x Loss for Three NMHC Compositions at Various NO_x Levels

NO_x, ppbv	Niwot NMHC Composition	ADMP NMHC Composition	EKMA NMHC Composition
	With Night NO_x Loss		
0.1	12.73	13.52	14.93
1	11.50	12.70	15.72
10	2.29	2.49	2.57
100	0.09	0.05	−0.13
	Without Night NO_x Loss		
0.1	22.21	23.66	26.99
1	20.08	23.12	33.46
10	9.12	11.41	16.22
100	4.33	4.60	0.75

Efficiency calculated in units of molecules of ozone produced per NO_x molecule consumed; NMHC is scaled to NO_x by 23.4.

However, measurements of NO_3 at night indicate that there are additional reactions involving NO_3 or N_2O_5 that may lead to a significant loss of NO_x [*Platt et al.*, 1984; *Noxon*, 1983], that is,

$$NO_3 + X \rightarrow \text{products} \quad (15)$$

$$N_2O_5 + Y \rightarrow \text{products} \quad (16)$$

where X and Y are as yet unspecified reactants. The possible candidates for X and Y may include propene, acetaldehyde, aerosols, clouds, and dew droplets [*Ehhalt and Drummond*, 1982; *Platt et al.*, 1984]. Obviously, inclusion of the nighttime sink will increase the NO_x loss. At the same time, the O_3 destruction would also be enhanced through (12) and (13). Consequently, the overall efficiency of O_3 production would decrease. At the present time the rate and the reaction products are not well understood. We can estimate the effect by assuming NO_3 formed in (12) is totally lost during the night.

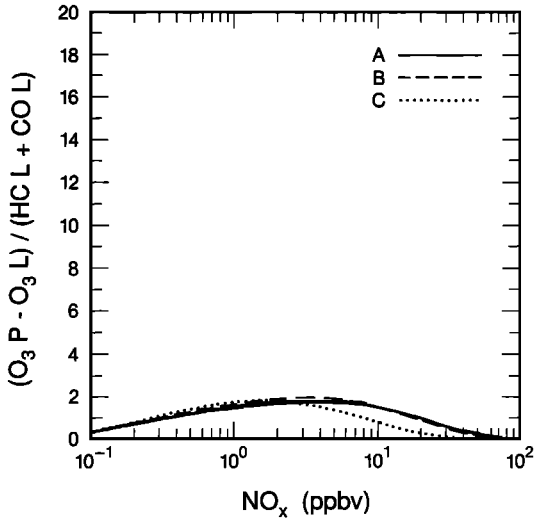

Fig. 10. Calculated O_3 production efficiency defined as net O_3 production versus loss of CO and hydrocarbons for three NMHC compositions: curve A, Niwot composition; curve B, ADMP composition; and curve C, EKMA composition. Here the nighttime loss of NO_x is included.

Figure 9 shows the O_3 production efficiency calculated under this assumption for three NMHC compositions. Remarkable reductions of the efficiency are apparent. The overall nonlinearity of the efficiency generally increases compared to Figure 4. A numerical comparison between Figure 9 and Figure 4 of the O_3 production efficiency at various NO_x levels is presented in Table 4. The negative efficiency at $NO_x = 100$ ppbv for the EKMA case, when the nighttime NO_x loss is included, indicates that O_3 loss exceeds O_3 production as result of the inclusion of (12) as O_3 loss. If we choose the ratio of O_3 production efficiency at $NO_x = 1$ ppbv to that at $NO_x = 10$ ppbv as a measure of the overall nonlinearity of the O_3 production efficiency, the overall nonlinearity is raised from 2.20 to 5.02, from 2.03 to 5.10, and from 2.06 to 6.12, for the three NMHC compositions, respectively. It should be noted that the effect would double if N_2O_5, instead of NO_3, is assumed to be removed totally.

As mentioned earlier, an interesting question is the degree of nonlinearity of O_3 production efficiency when NMHCs, instead of NO_x, are used as the reference precursor. To investigate the problem, we present three profiles in Figure 10 for the Niwot, ADMP, and EKMA compositions, respectively. They are O_3 production efficiencies calculated by using the sum of photochemical losses of CO, CH_4, and NMHCs, rather than the loss of NO_x. The nighttime loss of NO_3 is included in these calculations. We continue to use NO_x as the coordinate in Figure 10. It is obvious that the same nonlinearity will remain if NO_x is replaced by NMHCs as the horizontal coordinate, since they are scaled by a constant ratio. The new O_3 production efficiency is essentially linear in the range of NO_x value between 0.3 and 15 ppbv that is commonly found in rural air [*Fehsenfeld et al.*, 1988]. One can see that the efficiency varies between 0.5 and 2 in this NO_x range. Particularly for the two more realistic atmospheric NMHC compositions on a regional scale (Niwot and ADMP), the efficiency is confined to between 1 and 2. In other words, one to two O_3 molecules are produced for every molecule of CO or hydrocarbons that is oxidized. It appears that we may avoid the nonlinear problem in estimating regional O_3 budget by using CO and hydrocarbons as the reference precursor. However, while the nonlinearity problem is alleviated in this situation, one can no longer assume that loss rates of CO and hydro-

carbons are the same as their emission fluxes within the region where NO_x is between 0.3 and 15 ppbv. Because of their long photochemical lifetimes, substantial amounts of CO, CH_4, and other hydrocarbons emitted within the region will be transported and oxidized outside the region where the NO_x level is substantially below 0.3 ppbv and the nonlinearity is much greater.

Although the major objective of this study is to investigate the chemistry aspect of the nonlinearity of the O_3 production efficiency, it is clear that transport processes also play an important role. For example, transport processes tend to dilute secondary hydrocarbons and O_3 to values significantly lower than those calculated by our model. The net effect is to reduce the nonlinearity. By using a box model the effect of transport has been neglected in this study. A transport process that has a direct impact on the nighttime sink of NO_x is the formation of a shallow nocturnal inversion layer near the surface. In such a situation the exchange between the surface layer and the air aloft is inefficient. As a result, there usually is not enough O_3 in the surface layer to react with NO and NO_2 to form NO_3, especially at high NO_x levels. Therefore the high degree of nonlinearity shown in Figure 9 should be regarded as an upper limit. In this context we note that transport processes do not always reduce the degree of nonlinearity. For instance, transport of PAN, formaldehyde, and other similar secondary compounds from urban centers to rural areas will increase the nonlinearity by shifting ozone production from the former area to the latter. Obviously, a realistic study of the nonlinearity can best be accomplished by using a three-dimensional model with realistic transport parameterizations and emission sources.

IMPLICATIONS FOR OZONE BUDGET AND DISTRIBUTION

The existence of various degrees of nonlinearity relative to NO_x and NMHCs has several important implications for the budget and distribution of ozone and therefore its control strategy. An obvious implication can be readily seen from Figure 4 or 9. It shows that for a constant area-integrated NO_x emission flux, a concentrated emission source produces significantly less total ozone than a diffused emission source, except for NO_x levels less than 0.3 ppbv. This means that atmospheric transport processes play an important role in increasing the ozone production efficiency because the transport processes tend to diffuse concentrated sources [*Liu et al.*, 1987]. To evaluate accurately the budget and distribution of ozone, models with realistic transport processes are needed. This usually implies sophisticated three-dimensional models. On the other hand, if one's objective is to estimate an integrated regional ozone budget to within a factor of 3, a relatively simple approach can be adopted [*Liu et al.*, 1987]. For example, to estimate the total ozone production in the eastern United States, our results show that knowledge of the average concentrations of NO_x, CO, and hydrocarbons and the emission rate of NO_x is probably enough. These parameters can then be used in the formula $S = EP(L[NO_x])$, given earlier, to estimate the total ozone production. This is possible because the degree of nonlinearity in rural air is small enough to allow the ozone efficiency to be represented by an average value.

An interesting phenomenon of ozone distribution in the eastern United States is that rural ozone levels observed in the summer are either comparable to or frequently even higher than values of urban areas. This is surprising, because the levels of ozone precursors in urban atmosphere are usually an order of magnitude or more greater than those of rural air. For instance, NO_x mixing ratios in rural air in industrialized countries usually lie in the range between 0.2 and 20 ppbv [*Fehsenfeld et al.*, 1988], while the values of urban areas range from tens to hundreds of ppbv [e.g., *U.S. Environmental Protection Agency (EPA)*, 1983]. We believe that the nonlinearity shown in this study is a major factor that contributes to this phenomenon. This can be demonstrated by the following example.

For simplicity, we assume that the NO_x level is 5 ppbv in rural air and 50 ppbv over an urban area. In addition, we assume that the ratio of NMHCs to NO_x is 23.4 for the former and 2 for the latter. Adopting the ADMP hydrocarbon composition, from the profiles in Figures 4 and 5 the ozone production efficiency can be seen to be 14 in the rural air and 2 in the urban air. This compensates, to a large degree, for the factor of 10 disparity in the NO_x concentrations of the two areas.

It is clear that the nonlinarity will have important impacts on the control strategy for urban as well as rural oxidants. The factors that affect the degree of nonlinearity have to be considered in formulating an effective control strategy.

CONCLUSIONS

In this paper we have shown the dependence of the nonlinearity of the O_3 production efficiency, defined as net O_3 production divided by NO_x loss, on various parameters. These include the NMHCs composition, the ratio of NMHCs to NO_x, and the background abundance of natural hydrocarbons, CO and CH_4. Generally, the overall nonlinearity increases with both the reactivity of the hydrocarbon mixture and the ratio of NMHCs to NO_x. The increase of the nonlinearity is due (1) to enhancement of O_3 production through increased RO_2 and HO_2, (2) to reduction of NO_x loss through decreased OH at lower NO_x levels; and (3) to increase in O_3 destruction, that is attributed mainly to reactions of O_3 with alkenes, at higher NO_x levels. The background natural hydrocarbons, CO and CH_4 play a very important role in generating the nonlinearity. When CO, CH_4, and natural hydrocarbons are absent and NMHCs are scaled to NO_x, the O_3 production efficiency varies almost linearly with NO_x in most situations.

In addition to these findings, our model study also reveals the effects of combination reactions of peroxy radicals (HO_2 and RO_2) on the nonlinearity of O_3 production efficiency in the photochemical system. The radical combination reactions generally reduce the nonlinearity by substantially suppressing O_3 production efficiency at low NO_x levels.

When nighttime NO_x loss is included in the model calculation, O_3 production efficiency drops substantially for all levels of NO_x. The drop is due to increased loss of both NO_x and O_3. The overall nonlinearity of the O_3 production efficiency is increased by a factor more than 2 because of a relatively greater effect at higher NO_x.

The nonlinear property also exists if this O_3 production efficiency is defined as net O_3 production, divided by total loss of CO, CH_4, and NMHCs. In this case the O_3 production efficiency becomes almost linear in a NO_x range from 0.3 to 15 ppbv that is usually found in rural air [*Fehsenfeld et al.*, 1988]. However, the smaller nonlinearity of the new O_3 production efficiency in this NO_x range will not reduce the complexity in estimating regional O_3 budget, because the losses of CO, CH_4, and some NMHCs can not be approximated by

their regional emission fluxes as a result of their long photochemical lifetimes.

The nonlinearity has several important implications for the budget and distribution of ozone. It shows that for a constant area-integrated NO_x emission flux, a concentrated emission source produces significantly less total ozone than a diffused source, except at very low NO_x levels. This may be the major factor that contributes to the observed phenomenon in the eastern United States that rural ozone levels are comparable to values in urban areas. The nonlinearity also implies that atmospheric transport processes tend to increase the ozone production by diffusing concentrated NO_x sources.

By using a box model the present study is limited to examining the nonlinearity arising from photochemical processes. Moreover, many of the model calculations made were not realistic, because transport processes were omitted. It would be very valuable if this problem could be studied with a three-dimensional model that includes realistic parameterizations for transport processes.

Acknowledgments. We thank W. Stockwell for helpful discussions and for providing Figure 1*b*. This research has been funded as part of the National Acid Precipitation Program by the National Oceanic and Atmospheric Administration.

REFERENCES

Acid Deposition Modeling Project, Development and implementation of chemical mechanisms for the regional acid deposition model (RADM), Report to U.S. Environmental Protection Agency, Research Triangle Park, N. C., 1987.

Atkinson, R., and A. C. Lloyd, Evaluation of kinetic and mechanistic data for modeling of photochemical smog, *J. Phys. Chem. Ref. Data*, *13*, 315–444, 1984.

Carter, W. P. L., A. C. Lloyd, J. L. Sprung, and J. N. Pitts, Jr., Progress in the validation of a detailed mechanism for the photoxidation of propene and *n*-butane in photochemical smog, *Int. J. Chem. Kinet.*, *11*, 45–111, 1979.

Crutzen, P. J., The role of NO and NO_2 in the chemistry of the stratosphere and troposphere, *Annu. Rev. Earth Planet Sci.*, *7*, 443–472, 1979.

DeMore, W. B., D. M. Golden, R. F. Hampson, M. J. Kurylo, C. J. Howard, J. J. Margitan, M. J. Molina, and A. R. Ravishankara, Chemical kinetics and photochemical data for use in stratospheric modeling, Evaluation 7, *JPL Publ., 85-37*, 217 pp., 1985.

Dimitriades, B., and M. Dodge (Ed.), Proceedings of the Empirical Kinetic Modeling Approach (EKMA) Validation Workshop, *EPA Rep. EPA-600/9-83-014*, U.S. Environ. Prot. Agency, Research Triangle Park, N. C., 1983.

Dodge, M. C., Combined use of modeling techniques and smog chamber data to derive ozone precursor relationship, Proceedings of the International Conference on Photochemical Oxidant Pollution and Its Control, vol. II, edited by B. Dimitriades, *EPA-600/3-77.001b*, pp. 881–889, U.S. Environ. Prot. Agency, Research Triangle Park, N. C., 1977*a*.

Dodge, M. C., Effect of selected parameters on predictions of a photochemical model, *Rep. EPA-600/3-77-048*, U.S. Environ. Prot. Agency, Research Triangle Park, N. C., June, 1977*b*.

Ehhalt, D. H., and J. W. Drummond, The tropospheric cycle of NO_x, in *Chemistry of the Unpolluted and Polluted Troposphere*, edited by H. W. Georgii and W. Jaeschke, D. Reidel, Hingham, Mass., 1982.

Fehsenfeld, F. C., D. D. Parrish, and D. W. Fahey. The measurement of NO_x in the nonurban troposphere, in *Tropospheric Ozone*, edited by I. S. A. Isaksen, D. Reidel, Hingham, Mass., 1988.

Finlayson-Pitts, B. J., and J. N. Pitts, Jr., *Atmospheric Chemistry: Fundamentals and Experimental Techniques*, John Wiley, New York, 1986.

Fishman, J., S. Solomon, and P. J. Crutzen, Observational and theoretical evidence in support of a significant in-situ photochemical source of tropospheric ozone, *Tellus*, 31, 432–446, 1979.

Leighton, P. A., *Photochemistry of Air Pollution*, Academic, San Diego, Calif., 1961.

Leone, J. A., and J. H. Seinfeld, Comparative analysis of chemical reaction mechanisms for photochemical smog, *Atmos. Environ.*, *19*, 437–464, 1985.

Levy, H. B., II, J. D. Mahlman, W. J. Moxim, and S. C. Liu, Tropospheric ozone: The role of transport, *J. Geophys. Res.*, *90*, 3753–3771, 1985.

Liu, S. C., Possible effects on tropospheric O_3 and OH due to NO emissions, *Geophys. Res. Lett.*, *4*, 325–328, 1977.

Liu, S. C., M. McFarland, D. Kley, O. Zafiriou, and B. Huebert, Tropospheric NO_x and O_3 budgets in the equatorial Pacific, *J. Geophys. Res.*, *88*, 1360–1368, 1983.

Liu, S. C., M. Trainer, F. C. Fehsenfeld, D. D. Parrish, E. J. Williams, D. W. Fahey, G. Hübler, and P. C. Murphy, Ozone production in the rural troposphere and the implications for regional and global ozone distributions, *J. Geophys. Res.*, *92*, 4191–4207, 1987.

Lloyd, A. C., F. W. Lurmann, D. A. Godden, J. F. Hutchins, A. Q. Eschenroeder, and R. A. Nordsieck, Development of the ELSTAR photochemical air quality simulation model and its evaluation relative to the LARPP data base, *NTIS PB-80-188-139*, Natl. Tech. Inf. Serv., Springfield, Va., 1979.

Logan, J. A., M. J. Prather, S. C. Wofsy, and M. B. McElroy, Tropospheric chemistry: A global perspective, *J. Geophys. Res.*, *86*, 7210–7254, 1981.

Noxon, J. F., NO_3 and NO_2 in the mid-Pacific troposphere, *J. Geophys. Res.*, *88*, 11,017–11,021, 1983.

Platt, U. F., A. M. Winer, H. W. Biermann, R. Atkinson, and J. H. Pitts, Jr., Measurement of nitrate radical concentrations in continental air, *Environ. Sci. Technol.*, *18*, 365–369, 1984.

Seinfeld, J. H., *Atmospheric Chemistry and Physics of Air Pollution*, John Wiley, New York, 1986.

Singh, H. B., et al., Relationship between peroxyacetyl nitrate (PAN) and nitrogen oxides in the clean troposphere, *Nature*, *318*, 347–349, 1985.

Stockwell, W. R., J. D. Milford, G. J. McRae, P. Middleton, and J. S. Chang, Nonlinear coupling in NO_x–SO_x–reactive organic system, *Atmos. Environ.*, in press, 1988.

Trainer, M., E. Y. Hsie, S. A. McKenn, R. Tallamraju, D. D. Parrish, F. C. Fehsenfeld, and S. C. Liu, Impact of natural hydrocarbons on hydroxyl and peroxy radicals at a remote site, *J. Geophys. Res.*, *92*, 11,879–11,894, 1987.

Whitten, G. Z., H. Hogo, and J. P. Killus, The carbon bond mechanism: A condensed kinetic mechanism for photochemical smog, *Environ. Sci. Technol.*, *14*, 690–700, 1980.

U.S. Environmental Protection Agency, National air quality and emissions trends report, 1981, *EPA 450/4-83-011*, Research Triangle Park, N. C., 1983.

X. Lin, S. C. Liu, and M. Trainer, Aeronomy Laboratory, Environmental Research Laboratory, R/E/AL4, National Oceanic and Atmospheric Administration, 325 Broadway, Boulder, CO 80303.

(Received May 16, 1988;
revised September 23, 1988;
accepted September 27, 1988.)